

# Microslot NMR Probe for Metabolomics Studies

Hans Georg Krojanski,<sup>†</sup> Jörg Lambert,<sup>†,‡</sup> Yilmaz Gerikalan,<sup>†</sup> Dieter Suter,<sup>‡,§</sup> and Roland Hergenroeder<sup>\*†</sup>

ISAS—Institute for Analytical Sciences, Bunsen-Kirchhoff-Str. 11, 44139 Dortmund, Germany; IZMR—Interdisziplinäres Zentrum für Magnetische Resonanz, 44221 Dortmund, Germany; and Fachbereich Physik, Technische Universität Dortmund, Otto-Hahn Str. 4, 44221 Dortmund, Germany

**A NMR microprobe based on microstrip technology suitable for investigations of volume-limited samples in the low nanoliter range was designed. NMR spectra of sample quantities in the 100 pmol range can be obtained with this probe in a few seconds. The planar geometry of the probe is easily adaptable to the size and geometry requirements of the samples.**

Due to its high speciation performance, NMR is one of the major technologies for metabolic profiling.<sup>1</sup> NMR spectroscopy is a very information-rich analytical technique which gives comprehensive chemical information about the composition of unknown materials. The use of NMR spectroscopy as a tool for metabolomics, however, is limited by the sensitivity of NMR. Generally, one way to enhance the sensitivity is to increase the nuclear polarization, e.g., by dynamic nuclear polarization or optical pumping, and another approach is to improve the detection of the NMR signal.<sup>2</sup>

The optimum experimental setup for NMR on mass-limited biological samples is to dissolve the sample in the minimum volume of solvent to get the highest possible concentration, and to construct the smallest radio frequency (rf) coil that will enclose the sample.<sup>3</sup> The first microcoils that have been used for high-resolution <sup>1</sup>H NMR of nanoliter-volume samples were solenoidal coils.<sup>4,5</sup> The construction of solenoidal microcoils is feasible down to sizes of the order of 100  $\mu\text{m}$ . Further downscaling is currently hindered by practical problems. Therefore, planar microcoils, which are easier to scale down, were tested. Additionally, planar coil geometries allow for integration with microfluidic chips to realize a versatile “lab-on-a-chip”. Among the biggest challenges for planar helical coils is the relatively poor  $B_1$  rf field homogeneity and the static  $B_0$  field distortions induced by the windings of the microcoil.<sup>6</sup>

Recently, two new types of rf microcoils were used for high-resolution <sup>1</sup>H NMR, which are based on planar, electromagnetic

waveguides. Microstrip transmission line resonators were first used for surface coils in MRI by Zhang and co-workers, which gave also a brief theoretical description of the microstrip rf coil to guide coil design.<sup>7</sup> Van Bantum and co-workers introduced a stripline waveguide as the NMR detector.<sup>8</sup> It has been used for solid-state NMR<sup>9</sup> as well as high-resolution liquid-state NMR.<sup>10</sup> A slightly different approach was taken by Maguire and co-workers who used a small microslot in a microstrip waveguide that creates a pure series inductance as the rf coil.<sup>11</sup> As in conventional probes, lumped elements were used to build a resonance circuit and to match the system to the impedance of the spectrometer (50  $\Omega$ ). This approach is easily scalable to different sizes, and therefore we used this design to manufacture a microslot NMR probe for metabolomics NMR measurements on mass-limited samples. We used a femtosecond laser, which allows for very precise laser ablation for structures down to sizes of 1  $\mu\text{m}$ , and even below, with high aspect ratios. Femtosecond-laser ablation has the huge advantage that thermal damages and stresses degrading the microslot performance are avoided. The relatively thick copper film (>10  $\mu\text{m}$ ) is easily and precisely structured this way.

## EXPERIMENTAL SECTION

**Materials.** Deionized water (W. Schmidt GmbH), 99.9% labeled D<sub>2</sub>O, and <sup>2</sup>H-labeled chloroform (99.9%) (both from Aldrich Chemical) were used as solvents. Fused silica capillaries for capillary electrophoresis (CE) from CS-Chromatographie Service were used for the samples with inner diameters (i.d.) of 25, 50, 75, and 100  $\mu\text{m}$ ; the outer diameters (o.d.) were 360 and 363  $\mu\text{m}$  for the smallest and the three larger ones, respectively. Capillaries with i.d. 300  $\mu\text{m}$  (o.d. 400  $\mu\text{m}$ ) were employed for measurements of highly diluted samples (Hirschmann Laborgeräte). The variable capacitors (Voltronics Corp.) for probe building were nonmagnetic trimmer capacitors (NMAJ15HVE) with a range of 1–16 pF. The fixed capacitor was an 1 pF ATC chip capacitor (700 C series). The substrate used for microcoil fabrication was Rogers RT/duroid 5880 high-frequency laminate. The dielectric of this laminate is glass microfiber reinforced PTFE (thickness 3.175 mm) with electrodeposited copper on both sides (thickness 35  $\mu\text{m}$ ). For electrical connection, a semirigid coaxial cable (EZ 141-TP/M17) was used inside the probe (Huber + Suhner). The

\* To whom correspondence should be addressed. E-mail: roland.hergenroeder@isas.de.

<sup>†</sup> ISAS—Institute for Analytical Sciences.

<sup>‡</sup> IZMR—Interdisziplinäres Zentrum für Magnetische Resonanz.

<sup>§</sup> Technische Universität Dortmund.

(1) Griffin, J. L. *Philos. Trans. R. Soc. B* **2006**, *361*, 147–161.

(2) Fujiwara, T.; Ramamoorthy, A. *Annu. Rep. NMR Spectrosc.* **2006**, *58*, 155–175.

(3) Webb, A. G. *Prog. Nucl. Magn. Reson. Spectrosc.* **1997**, *31*, 1–42.

(4) Wu, N.; Peck, T. L.; Webb, A. G.; Magin, R. L.; Sweedler, J. V. *Anal. Chem.* **1994**, *66*, 3849–3857.

(5) Olson, D. L.; Peck, T. L.; Webb, A. G.; Magin, R. L.; Sweedler, J. V. *Science* **1995**, *270*, 1967–1970.

(6) Stocker, J. E.; Peck, T. L.; Webb, A. G.; Feng, M.; Magin, R. L. *IEEE Trans. Biomed. Eng.* **1997**, *44*, 1122–1127.

(7) Zhang, X.; Ugurbil, K.; Chen, W. *Magn. Reson. Med.* **2001**, *46*, 443–450.

(8) van Bantum, P. J. M.; Janssen, J. W. G.; Kentgens, A. P. M. *Analyst* **2004**, *129*, 793–803.

(9) van Bantum, P. J. M.; Janssen, J. W. G.; Kentgens, A. P. M.; Bart, J.; Gardeniers, J. G. E. *J. Magn. Reson.* **2007**, *189*, 104–113.

(10) Kentgens, A. P. M.; Bart, J.; van Bantum, P. J. M.; Brinkmann, A.; van Eck, E. R. H.; Gardeniers, J. G. E.; Janssen, J. W. G.; Knijn, P.; Vasa, S.; Verkuijlen, M. H. W. *J. Chem. Phys.* **2008**, *128*, 052202.

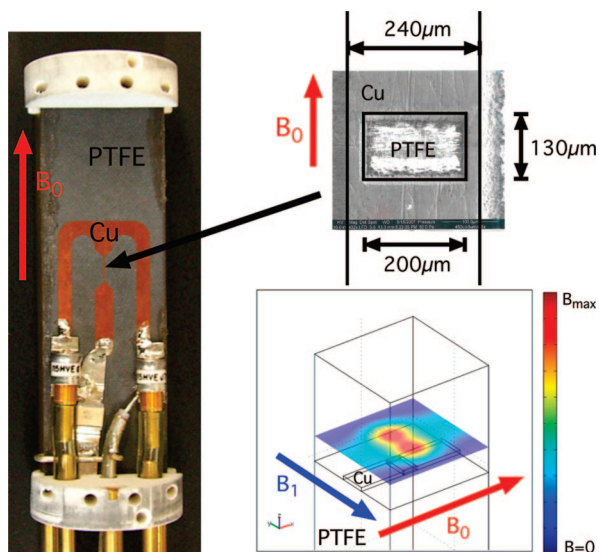


**Figure 1.** Left: Photograph of the upper part of the microslot probe. The black arrow points to the microstrip with the microslot at the center. Upper right: SEM picture of the microslot after the laser ablation. Lower right:  $B_1$ -field component in the vicinity of the microslot obtained by FEM simulation (linear scale from  $B = 0$  to  $B_{\max}$ ).  $B_0$  denotes the static magnetic field of the magnet, while  $B_1$  is the radio-frequency field generated by the microstrip.

photoresist used for chemical etching was AR-U 4040 Alresist (Alresist). The development of the exposed substrate was done with sodium hydroxide solution (7 g/L). The etching bath (Hema) consisted of sodium persulfate. For cleaning and polishing, deionized water, isopropanol, and abrasive paper with different grain sizes (Awuko) were used.

**NMR Probe Fabrication. Microslot Fabrication.** The microstrip and the support structure for soldering of the capacitors and the semirigid cable were chemically etched on one side of the Rogers substrate. First, the copper surface was cleaned with isopropanol and bidistilled water. Successively, the surface was polished to micron root-mean-square (rms) roughness. The remaining thickness of the film was approximately  $30 \mu\text{m}$ . After that, a thin film of photoresist was rolled up on the substrate. The mask for the structure and microstrip was pressed on the copper surface and was exposed for 25 s in a vacuum chamber to ultraviolet light. The development of the substrate was done in a sodium hydroxide bath for several seconds. After that, it was immersed in an etching bath that contained sodium persulfate for about 20 min. The micromachining of the microslot into the microstrip waveguide was made by femtosecond laser micromachining. A scanning electron microscope (SEM) picture of the microslot after the laser ablation is shown in the upper right-hand side of Figure 1. The left-hand side of this figure is a photograph of the upper part of the probe with the microstrip (black arrow), support structure (Cu), semirigid cable, and capacitors. The microstrip has a length of 6 mm, and the greatest length of the conductor from the impedance matching capacitors to the microslot is approximately 4 cm.

**Electrical Characterization.** The electrical measurements of the resonance circuit were first done with a vector network analyzer (Agilent AN 1287-1). The resonance circuit of the probe has a  $Q$ -factor of about 100, and standing wave ratios (SWR) of 1.001 are easily achievable. The dc (direct current) resistance of the structure (including the microstrip) is  $0.03 \Omega$  (Keithley 199

multimeter). After the probe was inserted into the magnet, the observation of the resonance of the probe circuit was performed with the built-in function of the Bruker spectrometer software (Topspin 2.0/2.1). To estimate the extension of the  $B_1$  field produced by the microslot, we used three-dimensional finite element (FEM) simulations (COMSOL Multiphysics with Electromagnetics module; Comsol). The lower right-hand side of Figure 1 shows the component of the magnetic field produced by the microslot which is perpendicular to the  $B_0$  field and to the axis along the microstrip. This component is the  $B_1$  field used in NMR to excite the nuclear spins, and it is also the component of the detected induced field produced by the spins. The figure shows a color map of the  $B_1$  field  $181.5 \mu\text{m}$  above the microslot (the center of most of the capillaries used). From FEM simulations, it can be seen that the  $B_1$  field does not exceed the length of the slot ( $130 \mu\text{m}$ ) and drops rapidly to zero along the microstrip (Figure 1). According to the simulations, the effective sample length of the NMR measurements is only  $150 \mu\text{m}$ , even if the filling height of the sample tube is several millimeters.

**Sample Preparation.** Individual sample tubes were cut as 1 cm pieces from fused silica capillaries. The sample tubes were cleaned in an ultrasonic bath with acetone, and then in deionized water for about an hour each. Before sample insertion, the capillaries were rinsed with deionized water and dried with compressed air. To fill the tubes they were dipped into the sample which was immediately sucked in by capillary forces. Kerr wax was used to seal the tubes after the insertion of the sample. The almost dumbbell-shaped sealed sample tube was then filed so that one flat surface including the outer surface of the capillary arose. This flat surface was used to position the sample tube on the microstrip. It was then taped down with adhesive tape. The positioning and the cleaning procedures were monitored with an optical microscope. Lysozyme was taken from Sigma, lyophilized powder, protein content 95%. The NCM460 (Incell Corp., San Antonio, TX) cell line was derived from normal human colon mucosal epithelium. Sucrose was taken from Aldrich, reagent grade 98%. DL-lactic acid lithium salt was taken from Aldrich, 95%.

**NMR Experiments.** NMR Experiments were carried out by using a 500 MHz (11.7 T) magnet, a four-channel Bruker Avance Spectrometer and a home-built probe including the circuit board with the microslot waveguide. In some cases comparison measurements with a conventional NMR probe (Bruker PAQXI 5 mm inverse probe) were performed.

## RESULTS AND DISCUSSION

**$B_0$  and  $B_1$  Homogeneity.** To characterize the probe, first a sample of a mixture of 5% deionized water and 95% deuterated water was measured. A typical spectrum is shown as the inset of Figure 2. In this example, 10.6 nL of water was filled into a capillary with an i.d. of  $300 \mu\text{m}$ , and an o.d. of  $400 \mu\text{m}$ . The rf pulse length was  $6.5 \mu\text{s}$  with 0.58 W output power at the probe, measured with an oscilloscope (LeCroy WavePro 950, 1 GHz, 16 GS/s). This corresponds to a rf conversion efficiency ( $B_1$  field per square root of power) of  $1.18 \text{ mT}/\sqrt{W}$ . For comparison, the Bruker PAQXI probe yields  $0.24 \text{ mT}/\sqrt{W}$ . The conversion efficiency is better for our microslot probe because of the smaller coil size. This has recently been shown for planar microresonators for electron spin resonance.<sup>12</sup>

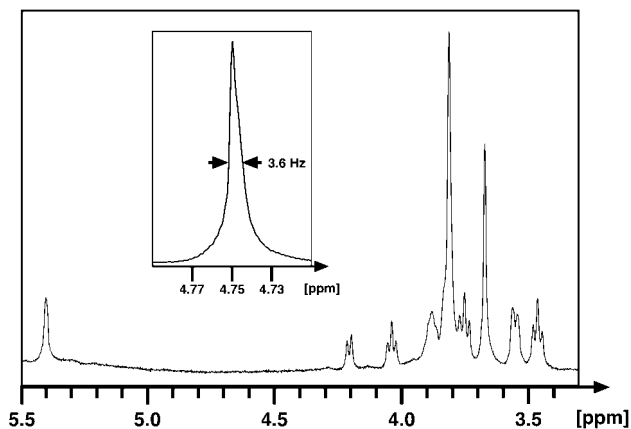


**Figure 2.**  $^1\text{H}$  spectrum of 2.28 nmol of sucrose in  $\text{D}_2\text{O}$ . The signal-to-noise ratio of the anomeric proton (on the far left side of the spectrum) is 69. The total acquisition time was 29 s with 16 accumulations. The inset shows a typical  $^1\text{H}$  spectrum of deionized water. The line width (full width at half-height) was calculated from a fit of a Lorentzian to the data. The solvent signal is absent in the sucrose spectrum because a presaturation water suppression technique was used.

A fit of a Lorentzian to the data results in a line width (full width at half-height (fwhh)) of 3.6 Hz (inset of Figure 2). No filter or apodization of the data was applied to the one-dimensional spectra. It was possible to get a line width of less than 1 Hz (fwhh), but only at the expense of a broad ( $\sim 50$  Hz) and distorted baseline of the resonance. In our experiments, we used the shim settings for obtaining Lorentzian-shaped resonance in water as a starting point for the shimming of other samples.

Nutation experiments were performed on water samples with different inner diameters of the sample tube to characterize the homogeneity of the  $B_1$  rf field of the probe coil. The resulting ratios of the signal amplitude at  $45^\circ$  and  $90^\circ$  flip angles are 97%, 94%, 83%, and 78% for inner diameters of the sample tubes of 25, 50, 75, and 100  $\mu\text{m}$ , respectively. This shows that the  $B_1$  field homogeneity gets worse with larger diameter of the samples, but it is in all tested capillaries still within reasonable limits for NMR spectroscopy. For comparison, a measurement of the  $45^\circ$  and  $90^\circ$  signal amplitude ratio yields 84% for the commercial Bruker PAQXI probe.

**Sensitivity.** For a given static magnetic field strength and sample concentration, the sensitivity of a NMR experiment is governed by the properties of the NMR probe. In NMR, the signal-to-noise ratio (SNR) is typically defined as the ratio of the height of a resonance of interest, divided by 2 times the root-mean-square of the noise floor. Usually, the SNR of the anomeric proton of sucrose is measured to quantify the sensitivity of a microcoil probe.<sup>13</sup> The spectrum of a sample with volume  $V_s = 10.6$  nL at 0.215 M concentration in  $\text{D}_2\text{O}$  is shown in Figure 2. To compare the sensitivity to the published literature data on NMR microcoils, the measured SNR is used to calculate the limit of detection (LOD)<sup>13</sup>

$$n\text{LOD}_m = \frac{3n\sqrt{t_{\text{Exp}}}}{\text{SNR}}$$

where the mole amount  $n$  refers to the portion of the sample within the detection volume and  $t_{\text{Exp}}$  is the total experiment time. To compare measurements done at different magnetic field

**Table 1. Measured Signal-to-Noise Ratios (SNR) and Calculated Limits of Detection ( $n\text{LOD}_m$ ) of Four Samples with Different Lactate Concentrations**

| $c$ (mol/L) | $n$ (nmol) | SNR   |               | $n\text{LOD}_m$ (nmol $\text{s}^{1/2}$ ) |               |
|-------------|------------|-------|---------------|--|---------------|
|             |            | CH    | $\text{CH}_3$ | CH                                       | $\text{CH}_3$ |
| 0.591       | 0.391      | 7.47  | 25.36         | 2.08                                     | 0.61          |
| 1.084       | 0.718      | 11.26 | 46.62         | 2.54                                     | 0.61          |
| 2.104       | 1.394      | 18.03 | 66.40         | 3.07                                     | 0.84          |
| 4.134       | 2.740      | 46.19 | 170.38        | 2.36                                     | 0.64          |

The effective sample volume was  $V_s = 663$  pL.

strengths  $B_0$ , a scaling to 600 MHz is used and therefore the SNR must be multiplied by 1.376 because of the  $\omega_L^4$  sensitivity scaling for inductive readout.<sup>14</sup> With an experiment time of  $16 \times 1.82$  s (16 accumulations), and a SNR of 69, the limit of detection is  $n\text{LOD}_m = 0.39$  nmol  $\text{s}^{1/2}$ . Maguire and co-workers measured a LOD of 3.05 nmol  $\text{s}^{1/2}$  for their probe (scaled to 600 MHz).<sup>11</sup> The main difference to our result is that they used the length of the sample for the calculation, whereas we used the estimated length  $l = 150$   $\mu\text{m}$  from FEM simulations to calculate the detection volume. Massin and co-workers manufactured a planar (spiral) microcoil on a glass substrate with etched microfluidic channels.<sup>15</sup> They used a slightly different figure of merit, the mass sensitivity per acquisition, and report a value of 88  $\mu\text{mol}^{-1}$  (scaled to 600 MHz) for the anomeric proton of sucrose with a Lorentz–Gauss resolution enhancement, which corresponds to a LOD of 34 nmol. For stripline probes, an experimental detection sensitivity of  $1.5 \times 10^{13}$  spins per  $\sqrt{\text{Hz}}$  (0.025 nmol/ $\sqrt{\text{Hz}}$ ) was calculated from the time domain sensitivity for a single scan proton spectrum of a 12 nL ethanol sample (measured at 600 MHz).<sup>9</sup>

To determine the limit of detection of metabolomic substances, we measured the SNR of a dilution series of lactic acid dissolved in  $\text{D}_2\text{O}$  for different concentrations  $c$  (Table 1). The amount of DL-lactic acid lithium salt that was dissolved in  $\text{D}_2\text{O}$  was measured with a precision balance (Mettler Toledo LabStyle 204). The signal-to-noise ratios of the CH and  $\text{CH}_3$  resonances in Table 1 were determined by dividing the height of the highest signal of the corresponding multiplet by 2 times the rms noise of the spectra.

In Table 1, the calculated limits of detection (LOD) are again scaled to 600 MHz. Due to the different multiplicities of the CH and  $\text{CH}_3$  signal, the LOD of the CH group is by a factor of 4 larger than the LOD of  $\text{CH}_3$ . From the mean of the measured data shown in Table 1 ( $n\text{LOD}_m(\text{CH}) = 2.51$  nmol  $\text{s}^{1/2}$ ,  $n\text{LOD}_m(\text{CH}_3) = 0.68$  nmol  $\text{s}^{1/2}$ ) and from the linear fits of the data (Figure 3) a factor of 3.7 is found.

The measured signal-to-noise ratios for CH and  $\text{CH}_3$  are shown in Figure 3 together with corresponding fits to the expected linear scaling of the SNR with lactate concentration. The fit results of Figure 3 show that the minimal concentration is  $c_{\text{min}} = 0.025$  mol/L for the lactate methyl signal. Therefore, with the same experi-

(11) Maguire, Y.; Chuang, I. L.; Zhang, S.; Gershfeld, N. *Proc. Natl. Acad. Sci.* **2007**, *104*, 9198–9203.

(12) Narkowicz, R.; Suter, D.; Niemeyer, I. *Rev. Sci. Instrum.* **2008**, *79*, 084702.

(13) Lacey, M. E.; Subramanian, R.; Olson, D. L.; Webb, A. G.; Sweedler, J. V. *Chem. Rev.* **1999**, *99*, 3133–3152.

(14) Hoult, D. I.; Richards, R. E. *J. Magn. Reson.* **1976**, *24*, 71–85.

(15) Massin, C.; Vincent, F.; Homay, A.; Ehrmann, K.; Boero, G.; Besse, P.-A.; Daridon, A.; Verpoorte, E.; de Rooij, N. F.; Popovic, R. S. *J. Magn. Reson.* **2003**, *164*, 242–255.

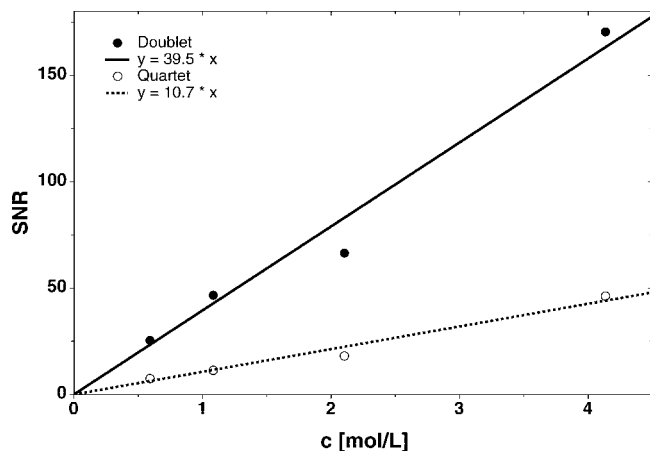


**Figure 3.** Signal-to-noise ratios (SNR) for the CH quartet and the CH<sub>3</sub> doublet of the lactate molecule for four different lactate concentrations. The minimal detectable concentration can be determined from the slope of the linear fits of the data. In each case, 16 accumulations were performed with an acquisition time of 0.79 s.

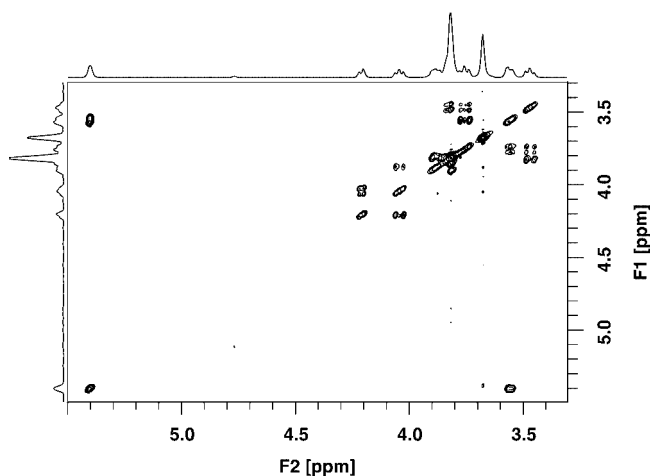


**Figure 4.** Two-dimensional COSY spectrum of 215 mM sucrose solution, obtained with the microslot probe. 256  $t_1$  increments of 8 scans were taken. The total measurement time was 81 min. An absolute value display was chosen with unshifted sine-bell apodization in both dimensions. Note: No drift corrections had to be applied between subsequent  $t_1$  increments.

mental conditions approximately 17 pmol of lactate ( $\approx 10^{13}$  molecules) can be detected with our microslot NMR probe.

**Two-Dimensional Experiments.** Figure 4 shows the two-dimensional COSY spectrum of 2.28 nmol sucrose dissolved in D<sub>2</sub>O in a capillary with an inner diameter of 300  $\mu\text{m}$  and an outer diameter of 400  $\mu\text{m}$ . The dimension of the FID data was 2048  $\times$  256, and 2 dummy scans and 8 accumulations were used. The total experiment time was about 81 min. To suppress the solvent signal, a 0.5 s long presaturation period with a rf field amplitude of about 610 Hz (compared to 38.5 kHz field amplitudes for the  $\pi/2$  pulse length) was used. It should be stressed that due to the favorable conditions for heat transport in the microstrip geometry presaturation powers that are 20 dB higher than in the standard high-resolution probes can be applied, resulting in a superior water suppression and obviating the need for more sophisticated water suppression schemes.

In Figure 5 two TOCSY spectra of lysozyme are shown that were measured with a conventional probe (bottom, Bruker PAQXI 5 mm inverse probe) and with our microslot NMR probe (top).

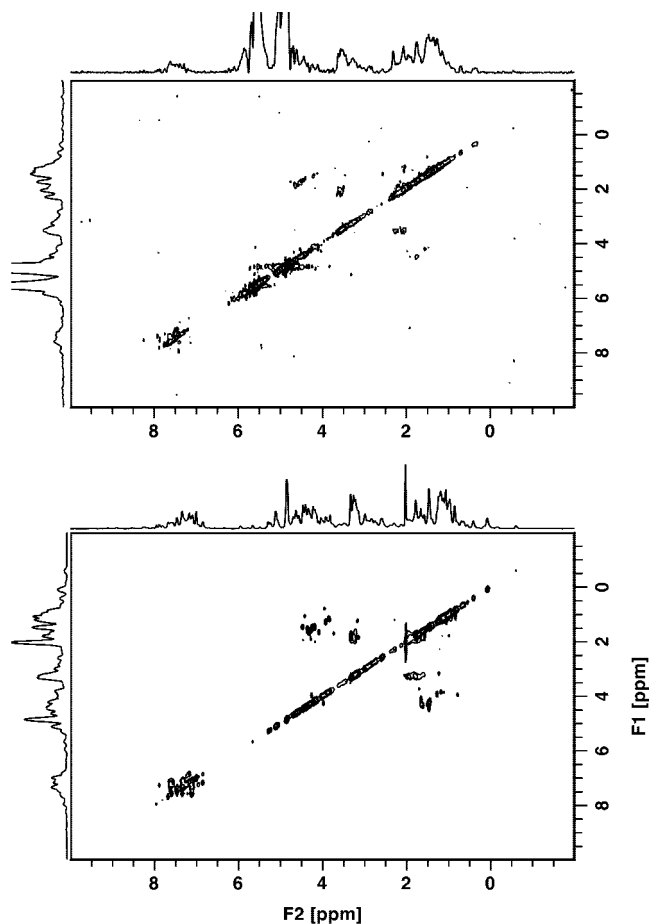


**Figure 5.** Comparison of two-dimensional TOCSY NMR spectra of lysozyme, measured with a conventional probe (bottom) and the microslot probe (top). The sample concentrations were 10 mg of lysozyme in 1 mL of D<sub>2</sub>O in both cases. 256  $t_1$  increments with 64 scans each were taken, resulting in a measurement time of 12 h. Weak cross peaks are missing in the microslot spectrum due to the slightly lower signal-to-noise ratio. The sample quantity, however, is by a factor of 56 600 lower.

The dimension of the measured data is 2048  $\times$  256 and 16 dummy scans and 64 accumulations were performed in each step of the experiment. The data were zero-filled in the F1 dimension (Figure 5) to 1024 points. Two unshifted sine-bell apodizations were applied. The lysozyme concentration was 10 mg in 1 mL of D<sub>2</sub>O for both measurements. Pure absorption phases were obtained with the States-TPPI technique.

The spin lock power level could be reduced by 10 dB as compared to a commercial probe for identical bandwidths. Nevertheless, the long isotropic mixing time of 80 ms leads to a considerable power deposition in the sample and corresponding sample heating. Moreover, at present there is no lock channel in our microslot probe to counteract the drift of the  $B_0$  field of 0.5 Hz/h. Both effects give rise to a signal drift over the long measurement time of 12 h. While the main features of the TOCSY spectrum measured with the PAQXI probe are also present in the spectrum measured with the microslot probe, the signal drift reduces the signal-to-noise ratio of weak crosspeaks below the noise floor (see Figure 5).

**Metabolomics Measurements.** Figure 6 shows NMR spectra of metabolites from noncancer colon mucosa cell line samples (NCM 460) measured with the Bruker PAQXI probe (top) and

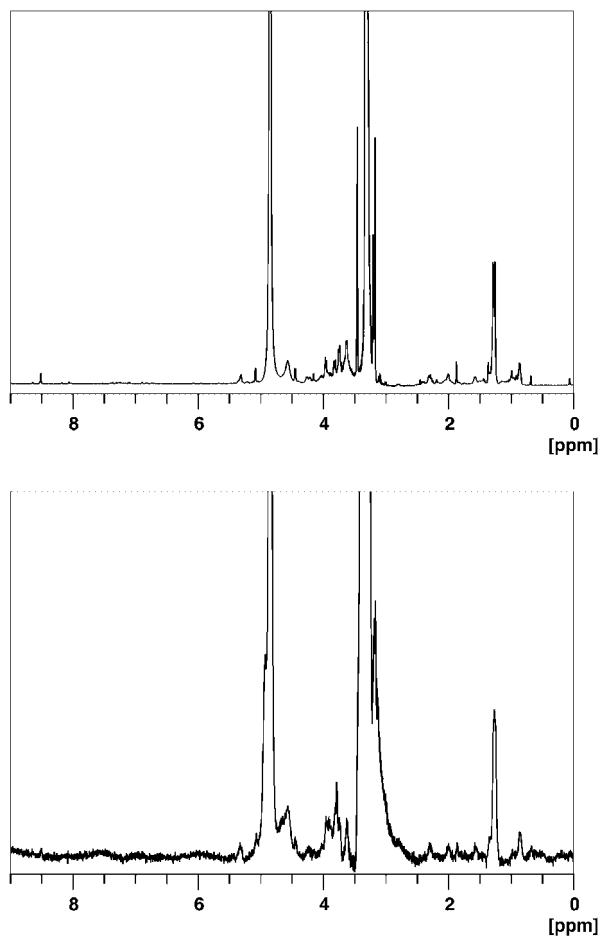


**Figure 6.** Spectra of a metabolite concentrate from the noncancer colon mucosa cell line NCM 460 measured with a conventional probe (top) and the microslot probe (bottom). 256 accumulations were taken for the commercial probe, and 324 accumulations for the microslot probe. In both cases, the total experiment time was 18 min, but the sample quantity for the microslot probe was by a factor of 56 600 lower.

our microslot probe (bottom). The concentration of metabolites was the same for both samples, but the sample volumes were different. In the PAQXI probe we used a standard 5 mm NMR tube with approximately 600  $\mu\text{L}$  sample volume. For the microslot measurement we used a capillary with an inner diameter of 300  $\mu\text{m}$  and the effective sample volume was 10.6 nL. The number of accumulations was 256 for the PAQXI measurement, and 324 accumulations for the microslot measurement. In both cases, the total experiment time was about 18 min.

We observed one broad background signal in the metabolomics measurements, probably originating from the fused silica capillary and from the glass microfiber reinforced PTFE dielectricum. The sample contains a range of components with small individual component concentrations. Hence, in contrast to the other samples, the background signal in this case dominates the appearance of the spectrum and has to be removed by using a cubic spline baseline correction.

In Figure 6, the spectrum obtained with the microstrip probe deviates minimally from the spectrum taken with the commercial probe. The absence of the doublet at 1.3 ppm in the microstrip spectrum is due to the higher signal line width arising from the missing susceptibility matching of the probe. Moreover, small-intensity peaks evident in the commercial probe spectrum are

missing in the microstrip spectrum (compare, e.g., the peaks at 8.5 ppm). In the microslot experiment, however, only 10.6 nL sample volume was used in contrast to 600  $\mu\text{L}$  for the commercial probe, i.e., 56 600 times less sample is needed for the microslot measurements.

**Conclusions and Future Directions.** We built a microslot probe by means of femtosecond laser ablation, which is capable of all basic NMR measurements for metabolomics studies. We achieved a reasonable resolution of a few hertz with this design. The limit of detection was 0.39 nmol  $\text{s}^{1/2}$  for sucrose (anomeric proton) and 0.68 nmol  $\text{s}^{1/2}$  for lactate ( $\text{CH}_3$ ). It is important to note that in our sensitivity calculations we did not employ matched filtering, which may help to optimize the SNR. In addition, we demonstrated that all important 2D NMR experiments for metabolomics can be performed with 5 orders of magnitude less sample compared to measurements with a conventional 5 mm probe.

To further improve the results of the more sophisticated 2D NMR experiments, a lock channel and temperature stabilization will be helpful. There are two methods to improve the resolution in future probe designs. One is the usage of zero-susceptibility materials instead of copper for the microstrip. The manufacturing of these materials is, however, difficult and the sensitivity suffers due to losses in the material compared to copper. Another possibility is the use of a susceptibility matching fluid like FC-43.<sup>5</sup> With our current probe design, this is not possible because we need the open access to the microslot for sample changes. However, if a fixed capillary with microfluidic access is used instead of individual short capillaries, it would be possible to use a matching fluid. Another advantage of a fixed capillary would be the possibility of high-throughput NMR measurements. The external microfluidic access would allow to inject well-defined picoliter sample quantities separated by spacers containing a suitable buffer solution. A related enhancement of the probe is the usage as the detector in capillary electrophoresis (CE). Previous CE-NMR experiments used solenoidal microcoils where the capillary flow is perpendicular to the  $B_0$  field. Hence the radial magnetic field of the capillary current distorts  $B_0$ , resulting in severe asymmetrical line broadening which dominates the broadening due to the finite residence time of the spins in the observe volume of the NMR probe.<sup>16</sup> In contrast, our microstrip NMR probe offers the possibility to orient the CE capillary parallel to the  $B_0$  field. Additional magnetic fields will then be perpendicular to the  $B_0$  field; i.e., no additional line broadening from electrophoretic flow is expected.<sup>16</sup> Currently, we are working on CE-NMR attachments to our probe as well as a microdrop injector for high-throughput measurements. The latter modification will also allow for a more precise effective sample volume determination. A different direction for the future development of the probe design would be the hyphenation of the planar microstrip probe with a microfluidic chip for in situ analysis of chemical reactions.

## ACKNOWLEDGMENT

Funding was provided within the framework of the “Pakt für Forschung und Innovation” of the Leibniz Society.

Received for review August 4, 2008. Accepted September 9, 2008.

AC801636A

(16) Olson, D. L.; Lacey, M. E.; Webb, A. G.; Sweedler, J. V. *Anal. Chem.* **1999**, *71*, 3070–3076.

## Microslot NMR Probe for Metabolomics Studies

Hans Georg Krojanski, Jo#rg Lambert, Yilmaz Gerikalan, Dieter Suter, and Roland Hergenro#der

*Anal. Chem.*, **2008**, 80 (22), 8668-8672 • DOI: 10.1021/ac801636a • Publication Date (Web): 22 October 2008

Downloaded from <http://pubs.acs.org> on December 14, 2008

### More About This Article

---

Additional resources and features associated with this article are available within the HTML version:

- Supporting Information
- Access to high resolution figures
- Links to articles and content related to this article
- Copyright permission to reproduce figures and/or text from this article

[View the Full Text HTML](#)